Effect of the loading rate on the fracture behavior of high-strength concrete

G. Ruiz[1], X.X. Zhang[1,2], R.C. Yu[1], J.R. del Viso[1], R. Porras[1], E. Poveda[1]
[1]*Universidad de Castilla-La Mancha, Ciudad Real, Spain;*
[2]*Harbin Engineering University, Harbin, China*

Abstract. This paper presents very recent results of an experimental program aimed at disclosing the loading rate effect on the fracture behavior of a high strength concrete. Twenty notched beams were tested using a hydraulic servo-controlled testing machine at five loading rates spanning six orders of magnitude in the loading point displacement rate (loading rate), from 1.74×10^{-5} mm/s to 17.4 mm/s. The results show that the work of fracture increases with the loading rate and so it ceases to be a material property in dynamic loading conditions. An analytical model is developed to take into account the rate-dependence of the material strength. It is based in a cohesive model endorsed with a viscous term dependent on the crack-opening rate. The model provides with an expression for the work of fracture that allows an excellent fitting of the experimental data. Furthermore, the fitting formula for the work of fracture gives the static specific fracture energy, which can really be considered a material property.

1   Introduction

High strength concrete (HSC) is very often used in modern complicated structures of considerable height and span, such as skyscrapers, high towers and large bridges. These are more vulnerable to damage caused by earthquakes, wind and blast loading owing to the fact that HSC is more brittle than normal strength concrete (NSC). Hence the construction industry is concerned on the dynamic fracture properties of HSC with regard to safety assessment and the design of modern structures.

Over the past few decades, researchers have mainly concentrated on the dynamic fracture behavior of NSC [1-11], and there have been different viewpoints concerning the effect of the loading rate (strain rate) on the fracture energy of concrete. It is generally accepted that the effect of the loading velocity is slight at low rates compared with the fracture energy variation at high loading rates [2], which leads some authors to conclude that fracture energy is rate independent at low loading rates [3, 12, 13]. Nevertheless, Oh [8] used three-point bend specimens to measure fracture energy at different low loading rates (from 8.3×10^{-4} mm/s to 0.83 mm/s) and his results show that the fracture energy and the nominal failure stress increase with the loading rate. Rossi and Toutlemonde [14] stated that this type of increase is mainly attributable to the presence of water in the micro-pore structure of the material. On the other hand, within the range of loading rates from

10^{-7} MPa/s to 30 GPa/s, the fracture energy of concrete increases greatly by a factor of 6-8 times [15]. Some researchers ascribe structural effects, like geometry of the specimen or inertia of the material, for such big magnification factors [16-19].

Much less information is available on the dynamic fracture behavior of HSC. Besides, applying conclusions obtained for NSC to HSC is not straightforward, since it is well known that the internal damage pattern of concrete varies as the strength increases [20]. For example, Schuler [21] measured the tensile strength and the fracture energy of HSC at high strain rates between 10 s^{-1} and 100 s^{-1}. A dynamic increase factor of 3 at a crack opening velocity of 1.7 m/s on the fracture energy was observed. Nevertheless, experimental data on the rate sensitivity of the fracture properties of HSC are very scarce. A need is felt for more research in this field that may throw light on the rate sensitivity of the fracture processes and on the causes that generate such sensitivity.

In order to gain additional insights into the loading rate effect on the fracture properties of HSC, in this paper we present three-point bending tests conducted at different loading rates. The results show that the fracture energy is approximately constant at low loading rates, and then increases at high loading rates. However, the peak load or the nominal failure stress constantly increases with the loading rate. This paper also provides a formulation for the rate-dependency of the fracture energy and of the nominal failure stress. It is based on a very simple cohesive model with a viscous term. The model may be helpful when simulating such rate dependency numerically.

This paper is structured as follows: the experimental procedure is given in section 2, in section 3 the results are presented and discussed. Section 4 presents the theoretical model and the analysis of the experimental data made according to the model. Finally, some conclusions are drawn in section 5.

2   Experimental procedure

2.1 Material characterization

A single high strength concrete was used throughout the experiments, made with an andesite aggregate of 12 mm maximum size and ASTM type I cement. Micro-silica fume slurry and super-plasticizer (Glenium ACE325 and B225) were used in the concrete composition. The water to cement ratio was fixed at 0.33. There was a strict control of the specimen-making process, to minimize scattering in test results. All of the specimens were cast in steel molds, vibrated by a vibrating table, wrap-cured for 24 hours, de-molded, and stored for 4 weeks in a moist chamber at 20 ℃ and 98% relative humidity until they were tested. Compressive tests were conducted according to ASTM C39 and C469 on 75 mm 150 mm (diameter×height) cylinders. Brazilian tests were also carried out using the same type of cylinders following the procedures recommended by ASTM C496. We made 8 cylinders, 4 for compression tests and 4 for splitting tests. Table 1 shows the char-

	f_c (MPa)	f_t (MPa)	E_c (GPa)
Mean	97	5.2	34
Std. Dev.	6	0.5	1

Table 1: Mechanical properties of the high-strength concrete.

acteristic mechanical parameters of the concrete determined in the various characterization and control tests.

2.2 Dynamic fracture tests

To investigate the effect of the loading rate on the fracture behavior of the high strength concrete, we carried out three-point bending tests on notched beams. The dimensions of the test beams were 100×100 mm ($B \times D$) in cross section, and 420 mm in total length. The initial notch-depth ratio was approximately 0.5, and the span was fixed at 400 mm during the tests. With regard to the measuring method for the specific work of fracture, W_F, we followed the procedures devised by Elices, Guinea and Planas [22-25] for getting the specific fracture energy but changing the loading rate. The tests were performed in position-control. Five loading rates were applied during the test from static or quasi-static level (1.74×10^{-5} mm/s, 5.50×10^{-4} mm/s) to dynamic level (1.74×10^{-2} mm/s, 5.50×10^{-1} mm/s and 17.4 mm/s). It should be noted that, in our tests, the kinetic energy of the specimen is very small and can be neglected compared with the fracture energy. Four specimens were used at each loading rate.

3   Results and discussion

Figure 1 shows typical load-displacement curves under different loading rates. It is obvious that the peak load increases with the increases in loading rates, while the critical deflection corresponding to the peak load almost remains constant. In regard to the stiffness of the beam, it also grows with the loading rate.
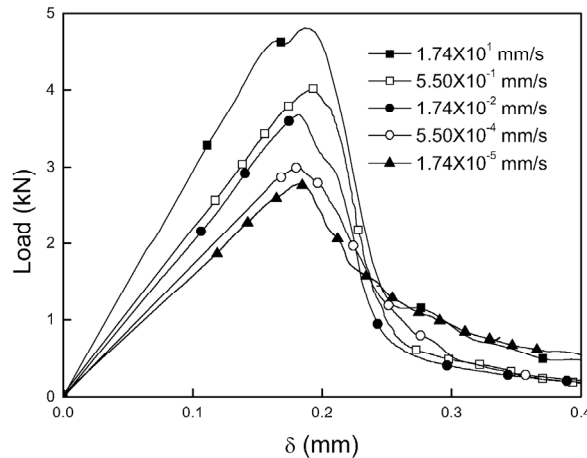
Fig. 1. Load-displacement curves at different loading rates.

$\dot{\delta}$ (mm/s)	P_{max} (kN)	W_F (N/m)
1.74×10^{-5}	2.9 [0.1]	135 [14]
5.50×10^{-4}	3.2 [0.4]	126 [6]
1.74×10^{-2}	3.6 [0.1]	133 [8]
0.55	3.8 [0.2]	155 [12]
17.4	5.0 [0.5]	200 [20]

Table 2: Test results for different loading rates.

3.1 Peak load and work of fracture

Table 2 arrays the mean results of four specimens for the peak load, P_{max}, and the work of fracture, W_F, measured at various loading rates. The values between brackets are the corresponding standard deviations. Please, note that we do not take W_F the same as the specific fracture energy G_F, since W_F in dynamic loading configuration ceases to be a material property, but it is rather the average work consumed per unit area. This will be clearly seen with the help of a theoretical model in section 4. Please, note that the peak load increases as the loading rate increases, whereas the work of fracture exhibits two different stages. First, W_F appears to be constant at low loading rates and then it increases at high loading rates. It is interesting to note that the value of W_F at the lowest loading rate is slightly greater than that obtained for the two following loading rates. Although it is clear that this effect can simply be attributed to experimental scatter, another possible explanation to this effect may be found in the humidity interchange of the specimen with the environment in the laboratory, since the crack propagation time lasted around eight hours.

3.2 Morphology of the crack surface

The resulting fracture surface of all the specimens tested in this research shows that the main crack propagates through aggregates. Besides, all the surfaces look the same regardless the velocity at which the specimen was tested. There is no hint of any increase in the generation of micro-cracks as the test velocity gets faster, which has been explained as the reason for the increase in the work of fracture by some researchers [2, 16, 18, 26, 27]. Instead, we think that, at the testing rates used here, it may be the movement of water though the network of pores of the bulk or the creation of new water surface as cracks advance that may explain the rate sensitivity that we find in our experiments. In the next section we are providing a validation for such hypothesis by analyzing the results of a theoretical model with a viscous component.

4 Model analysis

In order to take into account the strain rate effect observed in the experiments, we propose a dynamic cohesive law with a viscous term that follows the relation:

$$\sigma^D(w, \dot{w}) = \sigma^S(w)\, g(\dot{w}) \tag{1}$$

where $\sigma^S(w)$ is any convenient static cohesive law and $g(\dot{w})$ is a non-dimensional intensification factor whose expression is:

$$g(\dot{w}) = 1 + \left(\frac{\dot{w}}{\dot{w}_o} \right)^n \tag{2}$$

n being an index of rate dependence describing the degree of viscosity of the material, $\dot{w}$ the crack opening velocity and $\dot{w}_o$ a normalization parameter. The stress in the cohesive law is now related to the crack opening velocity, which implies that the model is going to represent rate-dependent effects due to the water present in the material. A similar rate-dependent cohesive law was proposed by Zhou et al. [28] for PMMA, with the difference that they applied the intensification factor to the openings while keeping the stresses untouched. As mentioned before, our tests show that the increase in the loading rate is followed by an increase in the load, especially in the peak load, but the displacements remain basically the same. Particularly, the displacement under the peak load remains approximately constant irrespective to the loading rate (please, see Fig. 1), which leads us to think that the viscous term should only affect the stress axis in the cohesive law.

We apply this cohesive law to a three-point bend test, assuming that two rigid-body sections are connected through a cohesive ligament at the central line, as shown in Fig. 2a. By so doing, the loading rate $\dot{\delta}$ can be directly related to the crack opening velocity $\dot{w}$ through the opening angle θ. We also assume, for the sake of simplicity, the linear cohesive law depicted in Fig. 2b. The stress has been regularized by the static tensile strength of the material, f_t^S, whereas we used the characteristic opening displacement, w_{ch} ($w_{ch} = G_F^S / f_t^S$, G_F^S being the static specific fracture energy) to write the openings in a non-dimensional way. Figure 2c and 2d plot non-dimensional load versus displacement curves given by the model for $n=0.25$ and $n=0.5$ varying the non-dimensional loading rate $\dot{\delta}/\dot{w}_o$ from 0 to 10^3. In both cases, the curves show similar trends to the ones observed in Fig. 1 for the experimental curves. In Figs. 2e and 2f, we plot the non-dimensional peak load $8P_{max}/(BDf_t^S)$ and the non-dimensional work of fracture W_F/G_F^S versus the loading rate $\dot{\delta}/\dot{w}_o$ for different values of n. Note that there is a transition point for $\dot{\delta}/\dot{w}_o$. Before that point, the peak load and the work of fracture decrease as the rate dependence index n increases for a fixed loading rate. After that point, this trend is reversed. The model allows deriving analytical expressions for the peak load and for the work of fracture as a function of the loading rate:

$$\frac{8P_{max}}{BDf_t^S} = 1 + \frac{1}{2^{n-1}(n+2)} \left(\frac{\dot{\delta}}{\dot{w}_o} \right)^n \tag{3}$$

$$\frac{W_F}{G_F^S} = 1 + \frac{2+(n+1)(n+4)}{2^n(n+1)(n+2)(n+3)} \left(\frac{\dot{\delta}}{\dot{w}_o} \right)^n \tag{4}$$
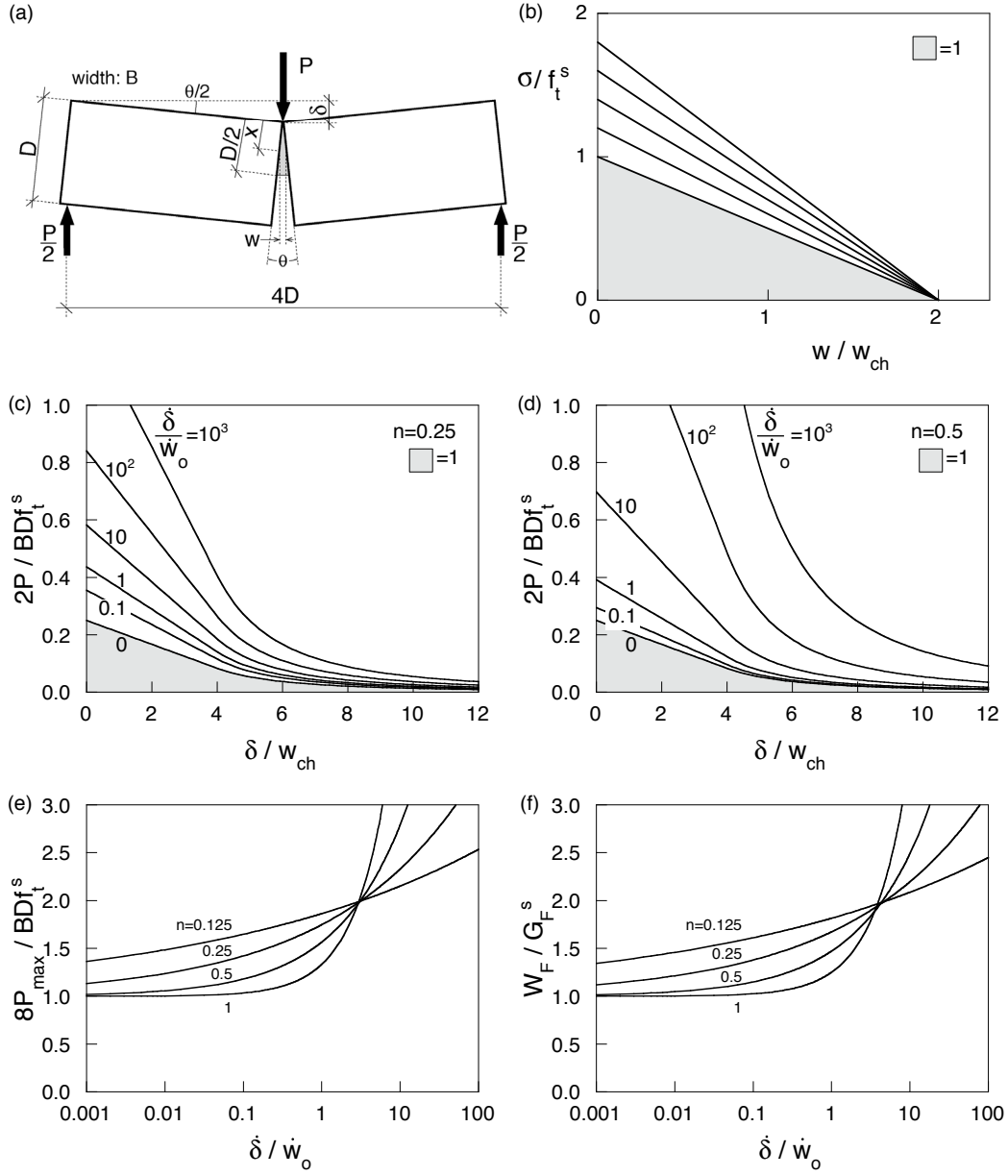
Fig. 2. Model description.

Please, notice that W_F in Eq. 4 does not represent the specific work of fracture consumed at any point of the ligament, but an average of such value along the ligament, since the cohesive model varies according to the crack opening displacement rate. This is why W_F can only be considered a material property in case the loading velocity be strictly zero, i.e. the test is performed statically.

In a general case, as the loading rate $\dot{\delta}$ is not directly related to the crack opening velocity $\dot{w}$, the non-dimensional values for the maximum load and the work of fracture are expected to follow as:

$$P_{max} / P_{max}^{S} = 1 + m_1 \dot{\delta}^{r} \qquad (5)$$
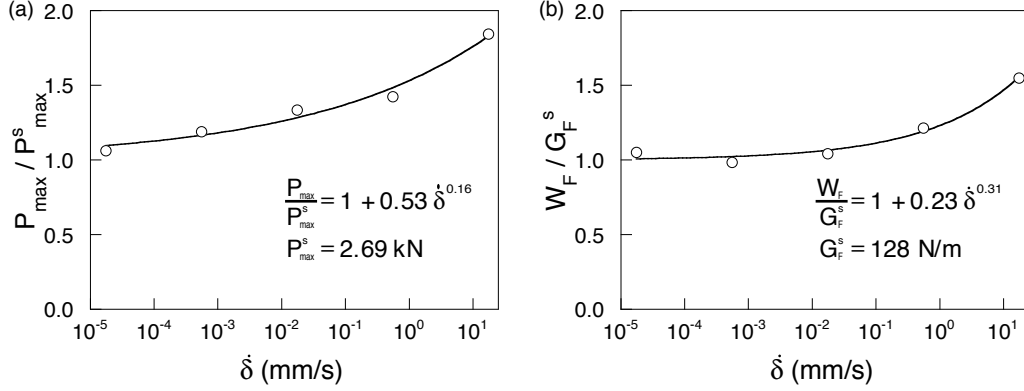
Fig. 3. Curves fitting the experimental data.

$$W_F / G_F^S = 1 + m_2 \dot{\delta}^s \tag{6}$$

where the parameters P_{max}^S, G_F^S, m_1, m_2, exponents r and s are adjusting parameters and can be obtained through fitting experimental results. In Fig. 3 we fit the above equations to the test data shown in section 2. It is noteworthy that the fitting also gives the static values of the maximum load and the static value of the work of fracture. Let us emphasize that G_F^S can be considered a true material property since it represents the specific fracture energy that would be obtained in a static test.

It is worth noting that the model also provides an explanation to the observed increase in W_F for very low displacement rates. Assuming that the desiccation of the specimen as it is tested implies that the index of rate-dependency n diminishes, the model predicts such an increase in W_F for low rates, as can be seen in Fig. 2f.

5   Conclusions

The fracture behavior of a high strength concrete under dynamic loading conditions was investigated in this study. We performed a series of three-point-bending tests on notched specimens to determine the amount of work used to break the specimen. The analysis of the experimental load-displacement curves was done according to the methodology proposed by Elices, Guinea and Planas [22-25], which minimizes experimental error. The loading rate varied from quasi-static level to a dynamic level, the order of magnitude varied from 10^{-5} mm/s to 10 mm/s.

The experimental results depend on the loading rate. The load-displacement curves reach bigger values of the load for higher loading rates, the displacement remaining basically the same, i.e. the curves are scaled in the load axis. Consequently, the maximum load increases with the loading rate within the interval of our study. The work of fracture starts to present a significant increase when the velocity of the displacement goes beyond 0.01 mm/s. The post-mortem analysis of the crack surface does not provide any evidence whatsoever of a different ex-

7

tent of micro-cracking for different loading rates, which could justify the rate sensitivity. On the contrary, we think that viscous effects due to the presence of water in the porous network of the concrete bulk may be responsible for the loading rate sensitivity described above.

In order to validate this hypothesis, we presented a theoretical model based on a viscous cohesive law. The cohesive stresses depend on the rate of the crack opening velocity, whereas the openings remain the same as in the static case. Under such conditions the expenditure of energy in the fracture process is not uniform along the crack path, since it depends on the crack opening velocity. This rate-dependent cohesive law is applied to a very simple case of two rigid half-beams united by a cohesive ligament and tested like our experimental beams. The model yields explicit expressions for the rate dependency of the peak load and of the specific work of fracture. The specific work of fracture in the presence of viscosity is just a ratio between the external work needed to propagate the crack and the area of the crack generated, but it is not anymore a property of the material. Expressions similar to the ones given by the model fit very well the experimental results. Particularly, the specific work of fracture for strictly static conditions can be derived from the set of experimental data. This value could be properly called a material property, the specific fracture energy, and only a methodology like the one followed in this paper can lead to obtain it. Nevertheless, according to our results, for small displacement velocities —below 0.01 mm/s for our concrete— the measured specific work of fracture is already very close to the strictly-static fracture energy.

Acknowledgments

References

[1]   J. Weerheijm, J.C.A.M. Van Doormaal, Tensile failure of concrete at high loading rates: New test data on strength and fracture energy from instrumented spalling tests, Int J Impact Eng 34 (2007) 609-626.

[2]   A. Brara, J.R. Klepaczko, Fracture energy of concrete at high loading rates in tension, Int J Impact Eng 34 (2007) 424-435.

[3]   H. Schuler, C. Mayrhofer, K. Thoma, Spall experiments for the measurement of the tensile strength and fracture energy of concrete at high strain rates, Int J Impact Eng 32 (2006) 1635-1650.

[4]   V. Bindiganavile, N. Banthia, Size effects and the dynamic response of plain concrete, J Mater Civil Eng 18 (2006) 485-491.

[5]   Y. Lu, K. Xu, Modelling of dynamic behaviour of concrete materials under blast loading, Int J Solids Struct 41 (2004) 131-143.

[6]   J.H. Yon, N.M. Hawkins, A.S. Kobayashi, Strain-rate sensitivity of concrete mechanical properties, ACI Mater J 89 (1992) 146-153.

[7] H.W. Reinhardt, J. Weerheijm, Tensile fracture of concrete at high loading rates taking account of inertia and crack velocity effects, Int J Fracture 51 (1991) 31-42.

[8] B.H. Oh, Fracture-Behavior of Concrete under High-Rates of Loading, Eng Fract Mech 35 (1990) 327-332.

[9] F.H. Wittmann, K. Rokugo, E. Bruehwiler, H. Mihashi, P. Simonin, Fracture energy and strain softening of concrete as determined by means of compact tension specimens, Mater Struct 21 (1988) 21-32.

[10] F.H. Wittmann, P.E. Roelfstra, H. Mihashi, Y.-Y. Huang, X.-H. Zhang, N. Nomura, Influence of age of loading, water-cement ratio and rate of loading on fracture energy of concrete, Mater Struct 20 (1987) 103-110.

[11] A.J. Zielinski, Model for tensile fracture of concrete at high rates of loading, Cement Concrete Res 14 (1984) 215-224.

[12] D. Birkimer, R. Lindemann, Dynamic tensile test of concrete materials, ACI Mater J 68 (1971) 47-49.

[13] J. Weerheijm, Concrete under impact tensile loading and lateral compression, PhD Thesis, Delft University of Technology, 1992.

[14] F. Toutlemonde, P. Rossi, Review of strain rate effects for concrete in tension. Discussion. ACI Mater J 96 (1999) 614-615.

[15] A. Zielinski, Fracture of concrete and mortar under uniaxial impact tensile loading, PhD Thesis, Delft University of Technology, 1982.

[16] G. Ruiz, A. Pandolfi, M. Ortiz, Three-dimensional cohesive modeling of dynamic mixed-mode fracture, Int J Numer Meth Eng 52 (2001) 97-120.

[17] J.C.A.M. van Doormaal, J. Weerheijm, L.J. Sluys, Experimental and numerical determination of the dynamic fracture energy of concrete, J Phys IV (1994).

[18] G. Ruiz, M. Ortiz, A. Pandolfi, Three-dimensional finite-element simulation of the dynamic Brazilian tests on concrete cylinders, Int J Numer Meth Eng 48 (2000) 963-994.

[19] F. Toutlemonde, Shock strength of concrete structures: from material behaviour to structure design, E.N.P.C., PhD thesis, Paris, 1994.

[20] D. Zhang, K. Wu, Fracture properties of high-strength concrete, J Mater Civil Eng 127 (2001) 86-88.

[21] H. Schuler, H. Hansson, Fracture behaviour of High Performance Concrete (HPC) investigated with a Hopkinson-Bar, J Phys IV (2006) 1145-1151.

[22] G.V. Guinea, J. Planas, M. Elices, Measurement of the fracture energy using 3-point bend tests. 1. Influence of experimental procedures, Mater Struct 25 (1992) 212-218.

[23] J. Planas, M. Elices, G.V. Guinea, Measurement of the fracture energy using 3-point bend tests. 2. Influence of bulk energy-dissipation, Mater Struct 25 (1992) 305-312.

[24] M. Elices, G.V. Guinea, J. Planas, Measurement of the fracture energy using 3-point bend tests. 3. Influence of cutting the P-δ tail, Mater Struct 25 (1992) 327-334.

[25] M. Elices, G.V. Guinea, J. Planas, On the measurement of concrete fracture energy using three-point bend tests, Mater Struct 30 (1997) 375-376.

[26] P.H. Bischoff, S.H. Perry, Compressive behaviour of concrete at high strain rates, Mater Struct 24 (1991) 425-450.

[27] I. Vegt, V.K. Breugel, J. Weerheijm, Failure mechanisms of concrete under impact loading. in: A. Carpinteri, P. Gambarova, G. Ferro, and G. Plizzari, (Eds.), Fracture Mechanics of Concrete and Concrete Structures, Taylor & Francis Group, Italy, Catania, 2007, pp. 579-587.

[28] F. Zhou, J.F. Molinari, T. Shioya, A rate-dependent cohesive model for simulating dynamic crack propagation in brittle materials, Eng Fract Mech 72 (2005)1383-1410.